Journal of Fluorescence
https://doi.org/10.1007/s10895-023-03189-0

RESEARCH

The Preparation and Nonlinear Properties Study of a Mixture of Polyurethane and Neutral Red Dye Solution

Kh. A. Al-Timimy[1] · H. A. Sultan[2] · Qusay M. A. Hassan[2] · C. A. Emshary[2] · Ali Qassim Abdullah[1] · Emad Abdul Reaz Arebi[1]

Received: 4 January 2023 / Accepted: 16 February 2023

Abstract
A mixture of polyurethane (PU) and neutral red (NR) dye solution is prepared. The nonlinear optical properties of the mixture of PU with NR dye solution are studied using a 473 nm laser beam of continuous fashion. The nonlinear refraction index of prepared material is determined via diffraction patterns and Z-scan. The diffraction patterns are calculated based on the Fresnel-Kirchhoff integral. Optical limiting of the prepared material is tested. All-optical switching occur in the sample using two low power visible laser beams.

Keywords Polyurethane · Diffraction ring patterns · Z-scan · All-optical swiching · Fresnel-Kirchhoff integral

Introduction

The search for materials having large nonlinear optical properties and short response times have led during the last three decades to the extensine research activities of different nonlinear optical organic, inorganic, liquid crystals [1–9] etc. Materials with nonlinear optical properties are popular due to their potential applications in development of photonic devices viz., optical data storage, optical communication, optical limiting, optical switching [10–16] etc. To study nonlinear optical properties of various materials, three techniques have been discovered or created since 1967. The first technique is the diffraction patterns [17], the second one is the thermal lens [18] and third one is the Z-scan [19]. The first one depends on the generation of diffraction ring patterns discovered in 1967 by Callen et al. [20], while the third one was pioneered by Sheik-Bahae et al. [21, 22] based on the deformation of the beam wave front. These two techniques have been used in the calcution of change of the medium refractive index, calculation of the nonlinear refractive index, both by calculating the maximum number of diffraction rings patterns at the high input power, while in the second technique the nonlinear refractive index and the nonlinear absorption coefficient can be calculated based on the closed and open aperture Z-scans.

During the last six years we have been engaged in using both techinques in the studying and investigating the linear and nonlinear optical properties of available materials [23–28], other materials with improved properties [29, 30], and developed new materials [31–42].

In this work a mixture of polyurethane (PU) and neutral red (NR) dye solution was used as a sample. The nonlinear optical properties of the mixture of PU and NR dye solution was studied via calculations of nonlinear refractive index, the nonlinear absorption coefficient, the optical limiting property using continuous wave (cw) laser beam at 473 nm wavelength, with Gaussian intensity distribution and low power. The experimental results were numerically determined using the Fresnel-Kirchhoff diffraction integral. All-optical switching property of the mixture of PU and NR dye solution was investigated using a controlling 473 nm and controlled 532 nm laser beams.

Experimental Details

Sample Preparation

To prepare a polyurethane (PU) doped with neutral red (NR) dye solution, methyl isocyanate mixed with neutral

✉ Qusay M. A. Hassan
qusayali64@yahoo.co.in

[1] Department of Physics, College of Science, University of Basrah, Basrah 61001, Iraq

[2] Department of Physics, College of Education for Pure Sciences, University of Basrah, Basrah 61001, Iraq

Published online: 24 February 2023

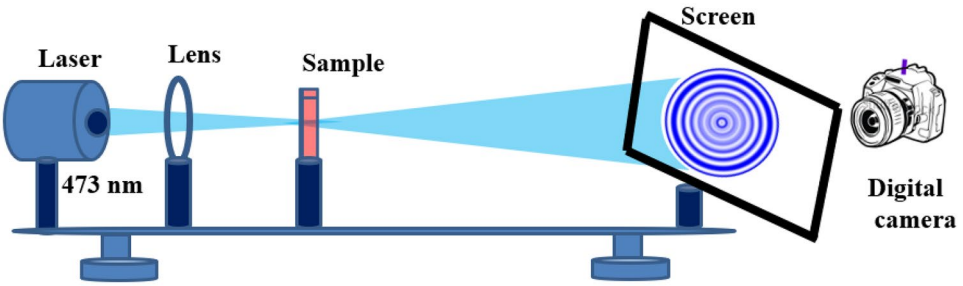

Fig. 1 Diagramatic sketch of obtaining diffraction ring patterns

red dye at weight ratio of 30%. Post mixing, the mixture was thoroughly mixed until a homogeneous mixture was obtained, until the mixture colour become dark red. To the mixture a first commercial polyester was added, the resultant mixture was thoroughly mixed until a squishy foam formed as a result of CO_2 gas release. The mixture viscosity increased slowly so that the foam harden, then it was left 24 h at room temperature to ensure the complete hardness. The final material is the PU doped with NR dye. The velocity of mixing and mixing ratio are vital parameters in obtaining homogeneous mixture otherwise a chemical rection resulted instead of physical mixing (polymer blend). A solution resulted when the PU doped with NR dye dissolved in dimethyl sulfoxide.

Experimental Setups

To produce diffraction patterns the experimental set-up shown in Fig. 1 was used. A cw 473 nm laser beam emitted by a solid state laser device (type SDL-473-050 T) was used. The power of laser beam was varied in the range 0—66 mW, with spot radius of 1.5 mm (at $1/e^2$) when beam leaves the device output mirror. The laser beam was focused to 19.235 μm at the entrance of the sample cell using a positive lens of focal length of 50 mm and a 1 mm thickness sample glass cell. The produced diffraction patterns fall on a 30 × 30 cm semitransparent screen which was 85 cm from the sample cell exit plane registered by a digital camera of velocity of 1/32 s.

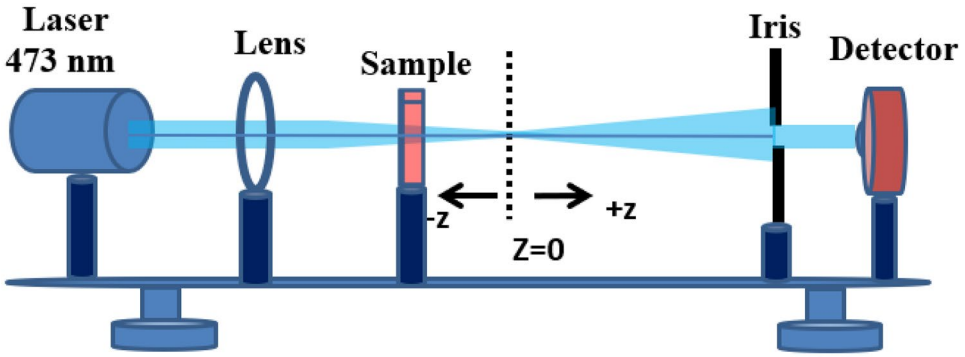

Fig. 2 Diagramatic sketch for carrying out the closed aperture Z-scan experiment

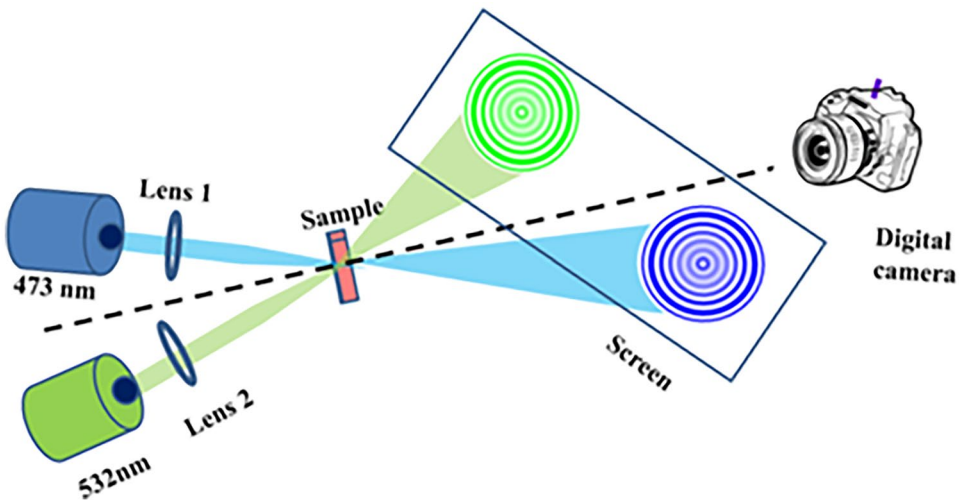

Fig. 3 Diagramatic sketch of all-optical switching

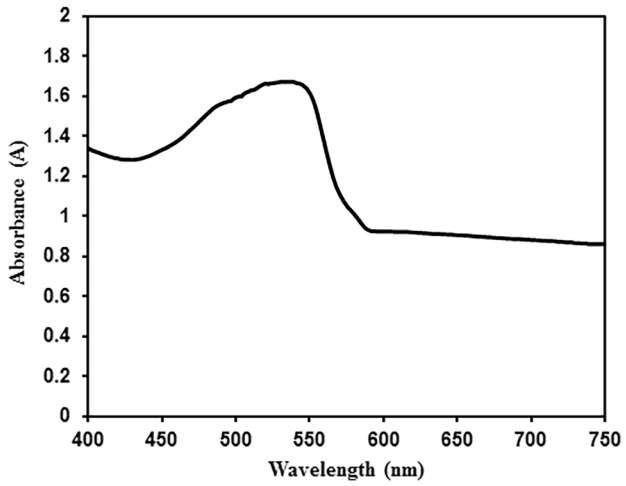

Fig. 4 Absorbance(A) spectrum in the mixture of PU and NR dye solution

The Z-scan experiments were perfomed using Fig. 2 and the same type laser beam. Here the measurements were made by keeping the power input constant, and the sample cell was translated the distance (-z)—(+ z) using a movable stage where the lens focus is at z = 0. Using a power meter in place of the screen covered with 2 mm diameter circular iris a closed aperture CA Z-scan resulted, so that the area of the spot size varied as it fall on the iris that vary the transmitted beam power registered by the detector, and by using another positive lens instead of the iris we have the open aperture OA Z-scan. In both experiments the transmitted powers of the laser beam were measured against the sample position (± z).

The optical limiting property of the mixture of PU and NR dye solution was examined via the same laser beam, the same cell, the same lens and fixing the sample position in the valley property of the CA-Z-scan and the measurements were made by changing the input power and recording the corresponding transmitted laser beams powers using the same power meter respectively.

The all-optical switching experiments were conducted using Fig. 3 with two laser beams of the same properties except that the first one, 473 nm, was used as the irradiation or controlling beam while the second one, 532 nm, (type SDL-532-050 T) nm beam was the controlled beam. Both laser beams were focused at the sample cell by two identical glass, 20 cm focal length, lenses so that the spot sizes of the laser beams equals 76.94 μm and 86.54 μm for the 473 nm and 532 nm beams respectively. The cross-passing technique [43, 44] was used where the two laser beams were focussed.

Results and Discussion

Measurements Absorption Coefficients

To measure the absorption coefficient of the mixture of PU and NR dye solution at room temperature in the UV–vis. spectrum a spectrophotometer (type England- Jenway-6800) was used. Figure 4 shows the absorbance (A) spectrum of the mixture PU and NR dye solution versus the wavelength through UV–vis. To calculate the sample absorption coefficient (α), the data of Fig. 4 and the following equation [45]

$$\alpha(cm^{-1}) = 2.303\frac{A}{d} \quad (1)$$

were used. A is the absorbance at wavelength, λ, and d is the sample thickness. For A_{473} and A_{532} of 1.45,1.67 respectively and d = 0.1 cm, α_{473} and α_{532} values are 33.39 cm^{-1}, 38.46 cm^{-1} respectively.

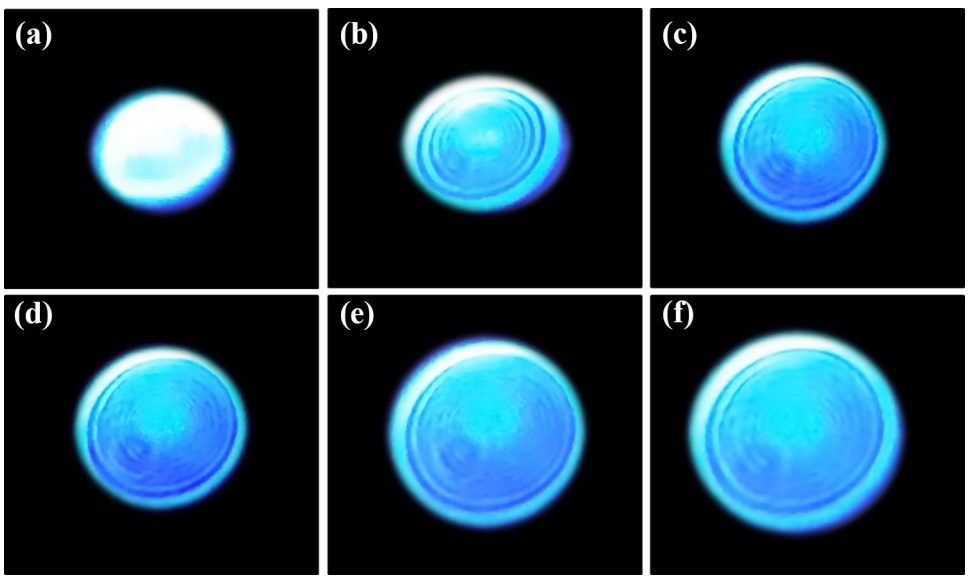

Fig. 5 Images of the temporal evolution of a chosen far field diffraction patterns in mixture of PU and NR dye solution at 61 mW, (m sec): **a** 0, **b** 100, **c** 200, **d** 500, **e** 850, **f** 1000

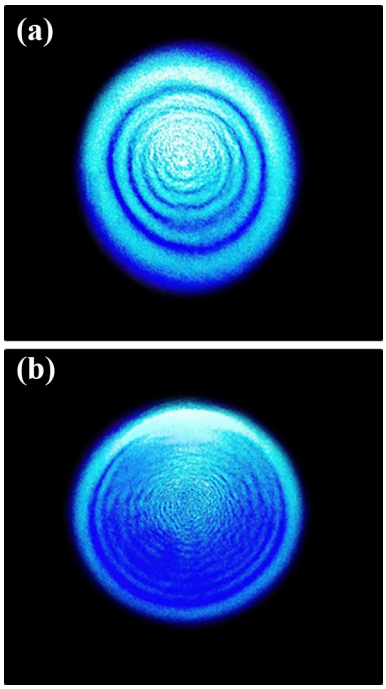

Fig. 6 Images of dependence of the far field diffraction patterns on the beam wavefront **a** convex, **b** concave in mixture of PU and NR dye solution at power input 61 mW

Diffraction Patterns

Figure 5 shows the temporal variations of diffraction patterns formed on the semitransparent screen 85 cm away from the sample cell. The diffraction patterns are understood to be induced by the spatial self-phase modulation arised from the laser induced refractive index change. The pump laser beam have Gaussian intensity profile induces phase shift, Δφ, with a bell-shaped transverse profile. For each point, say ρ_1, on the beam wavefront there always exist another point, say ρ_2, with the same slope. Maximum constructive and destructive interfereances occurs when $\Delta\varphi(\rho_1)$ and $\Delta\varphi(\rho_2)$ are related as $\Delta\varphi(\rho_1) - \Delta\varphi(\rho_2) = m\pi$ for m being even or odd integers for constructive and destructive interferences respectively so that with the increase of input power series of circular rings resulted i.e., diffraction patterns. As time pass, the spot size increased in area due to self-defocusing. By the continuous lapse of time, the spot splits into rings, the rings number increases as time lapse until it settle at steady state number to a maximum number of rings related to the maximum power input. It is believed that diffraction.

patterns type depends on the beam wave front. i.e., the interaction of the beam with the nonlinear material is beam wave front dependent [46, 47]. Figure 6 shows the beam wave front effect on the diffraction patterns (a) convex and

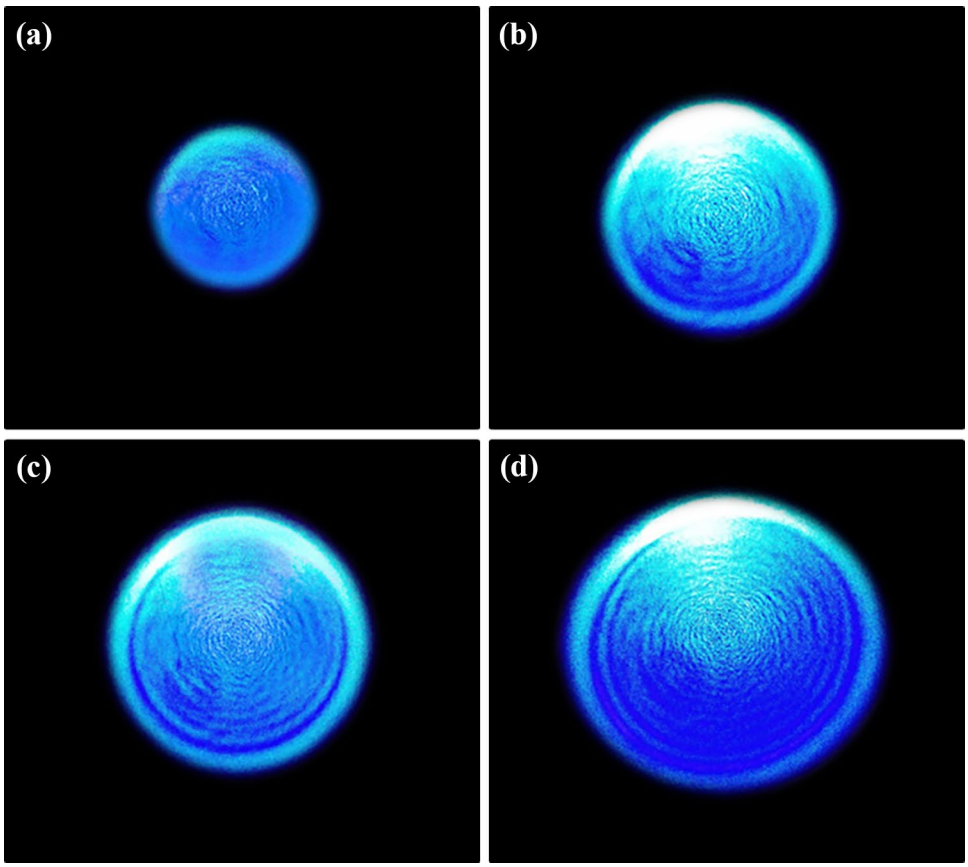

Fig. 7 Images of power dependence of the far field diffraction patterns in mixture PU and NR dye solution (mW) in the far field: **a** 17, **b** 27, **c** 42, **d** 61

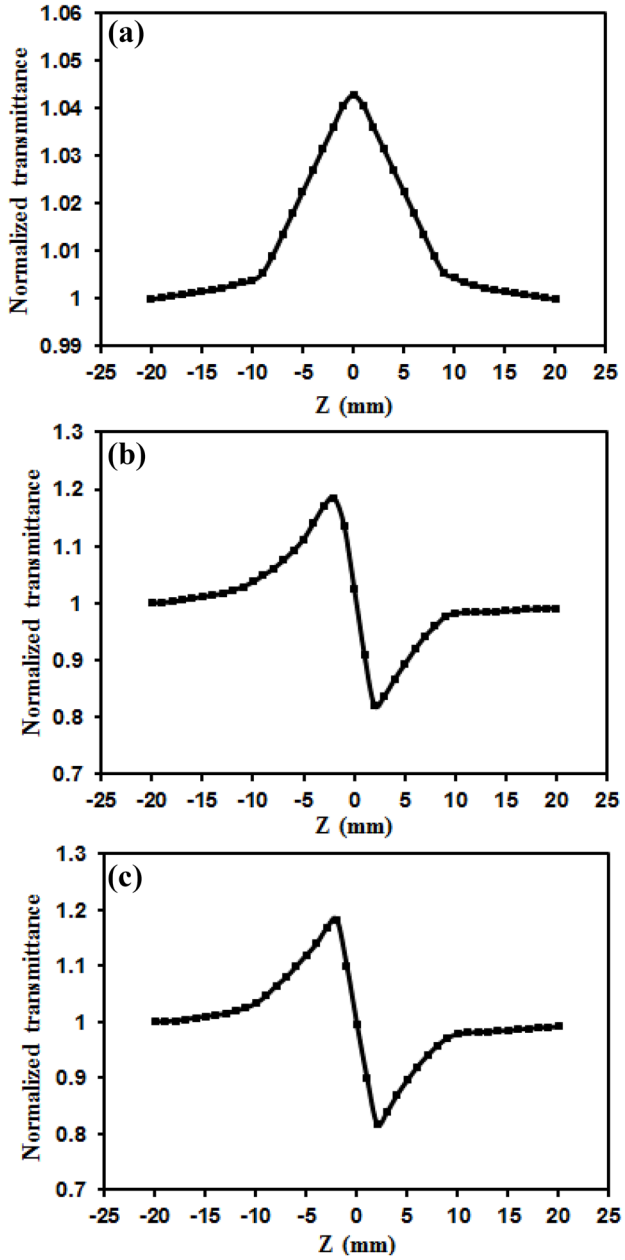

Fig. 8 Normalised Z-scan data **a** OA, **b** CA, and **c** devision of (**b**) by (**a**) in the PU and NR dye mixture solution, at input power 5 mW

(b) concave beams. By slowly increase the input power falling on the sample the effects are shown in Fig. 7 where the rings number, area of each ring pattern and the asymmetries in the upper part of the far field diffraction patterns, all increases monotonically as the power input increased. Also external ring in every pattern are intense compare to the inner ones due to self-defocusing.

Z-scan

Due to carrying the OA:Z-scan in PU and NR dye solution, the results obtained displayed in Fig. 8a. It is noted that the Fig. 8a has a peak at z = 0, an indication of absorption saturation and that the sign of the nonlinear absorption coefficient is negative. By carrying the CA Z-scan, the results shown in Fig. 8b was obtained. It is noted from the Fig. 8b that it has a peak succeeded by a valley, an indication of self-defocusing occurrence and that the sign of nonlinear refractive index is negative. Figure 8c is the result of dividing the CA: by OA: Z-scan data to give the pure nonlinear refractive index. The nonlinearity in the present study is thermal in nature as result of using the cw beam.

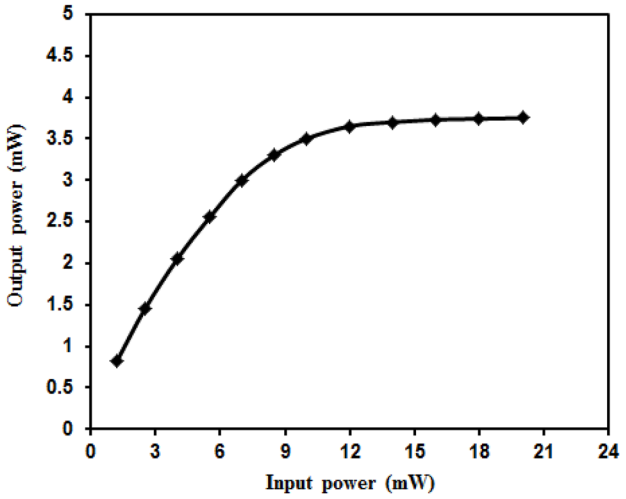

Fig. 9 The optical limiting property of the mixture of PU and NR dye solution

Optical Limiting

To measure the chracterstics optical limiting of the prepared solution of PU and NR dye the incident power, P_{in}, and corresponding transmitted one, P_{out}, through the sample were measured and the Fig. 9 shows the relation between them. Where it is noted from Fig. 9 that at low power input the relation between P_{out} and P_{in} is linear. By increasing P_{in}, relation of P_{in} against P_{out} become nonlinear then it switch to constant P_{out} against P_{in} at high power input.

All-optical Switching

When the 532 nm or the controlled laser beam, with low input power, fall on the sample, no diffraction patterns resulted as shown in Fig. 10S1(a) i.e., no rings appears even when increasing its power. When the 473 nm or the controlling beam fall on the sample alone diffraction patterns appears even at low power input,see in Fig. 10S1(c). When both beams fall on the sample diffraction patterns of the 532 nm beam (Fig. 10S1(b)) resulted due to the spatial cross-phase modulation together with spatial-self phase modulation [48, 49]. By increasing the power input of the

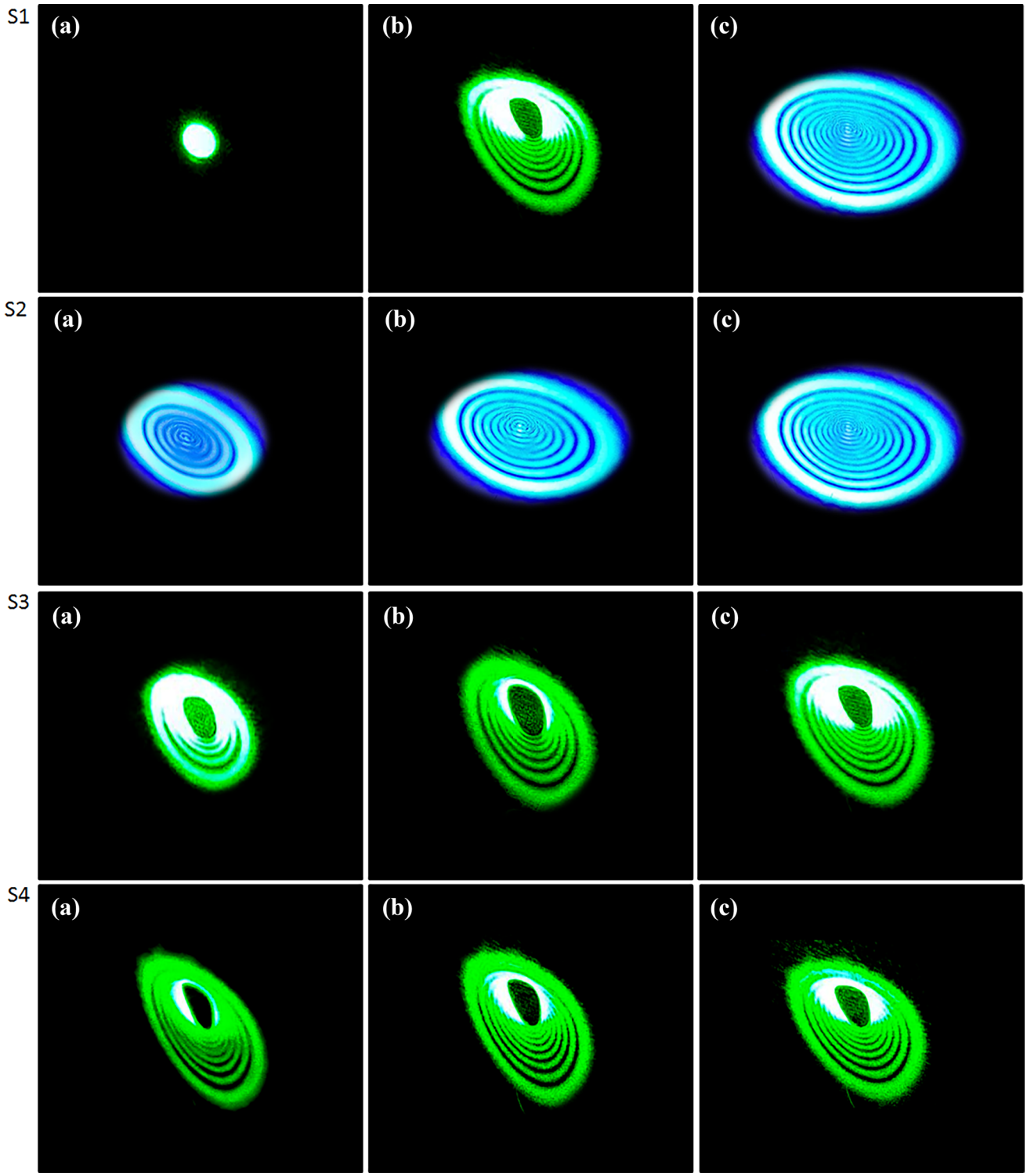

Fig. 10 **S1**(a) no rings appears when the controlled 532 nm beam incident alone on the sample at moderate input power, **S1**(b) and (c) rings appears as the controlling 473 nm beam traverses the sample together with the controlled beam. Figure **S2** shows the controlling beam effect on the blue patterns, **S3** shows the controlling beam effect on the controlled beam patterns, and **S4** shows effect of the controlled beam on its patterns

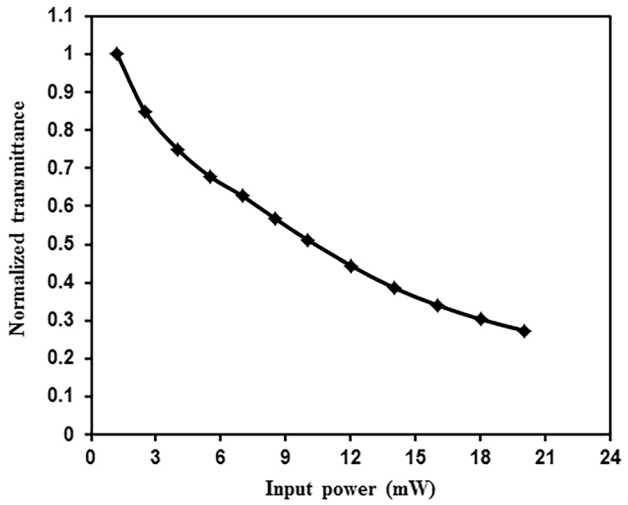

Fig. 11 Normalized transmittance against input power in the mixture of PU and NR dye solution

473 nm beams the area of each ring pattern, the number of rings, and the asymmetry of the blue diffraction patterns and green diffraction patterns increases as it's power input increases as shown in Fig. 10S2, S3 respectively. By increasing the controlled 532 nm beam power input, increase its diffraction patterns intensity only i.e. it does not affect the green diffraction patterns number of rings neither the area of each diffraction patterns nor the asymmetries as shown in Fig. 10S4.

Calculations of the Nonlinear Refractive Index Due to Diffraction Patterns and Z-scan

In the case of diffraction patterns, the nonlinear refractive index of the mixture PU and NR dye solution can be evaluated based on the number of diffraction rings at the highest input power. The relation between the change of the medium refractive index, Δn, and input intensity I, can be written as follows [50]:

$$n_2\left(\frac{cm^2}{W}\right) = \frac{\Delta n}{I} \tag{2}$$

I can written as follows:

$$I\left(\frac{W}{cm^2}\right) = \frac{2P}{\pi\omega^2} \tag{3}$$

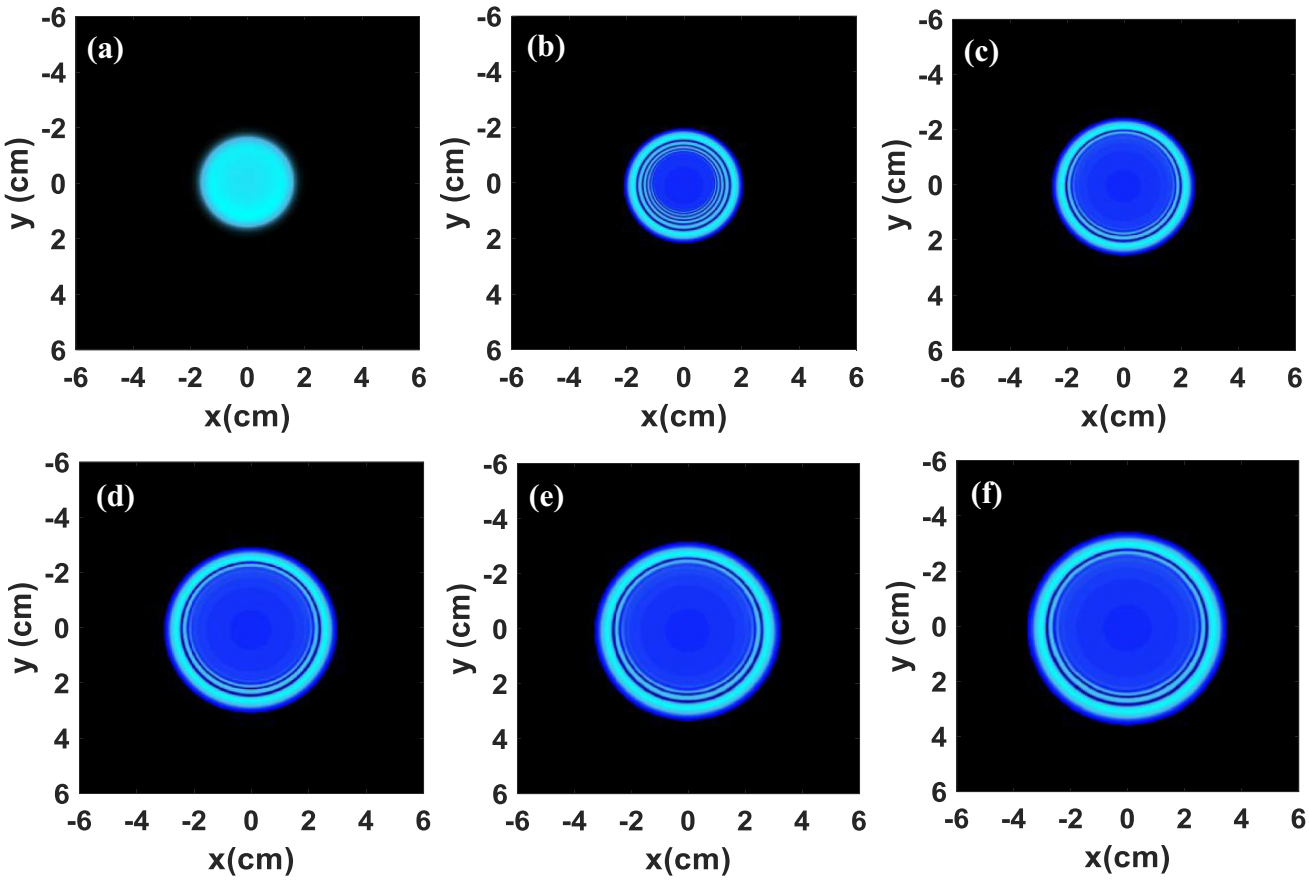

Fig. 12 Theoretically calculated temporal variations at far field of a chosen far field diffraction pattern, msec: **a** 0, **b** 100, **c** 200, **d** 500, **e** 850, **f** 1000 in mixture of PU and NR dye solution at 61 mW

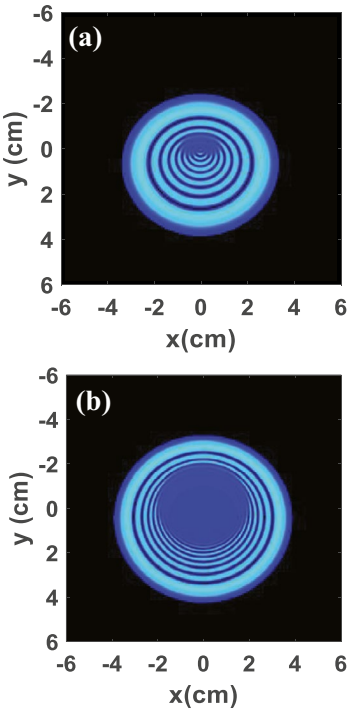

Fig. 13 Theoretically calculated variations of the far field diffraction patterns with the wave front effect of beam for **a** convex wave front and **b** concave wave front, at the far field in polyurethane at 61 mW in the mixture of PU and NR dye solution

P is the maximum beam power incident on the sample and ω is its radius. Δn can be related to the maximum number of rings,N, wavelength,λ, and sample thickness, d,as follows:

$$\Delta n = \frac{N\lambda}{d} \tag{4}$$

For N=8, λ = 473 nm, P = 61 mW, ω = 19.235 μm, d = 0.1 cm so that $\Delta n = 3.78 \times 10^{-3}$ and $n_2 = 3.99 \times 10^{-7}$ cm^2/W respectively.

In the Z-scan case nonlinear refractive index, n_2, can be determined based on the following relation [22]

$$n_2\left(\frac{cm^2}{W}\right) = \frac{\Delta\varphi\lambda}{2\pi L_{eff} I} \tag{5}$$

While the nonlinear coefficient of absorption, β, is calculated using the following relation

$$\beta\left(\frac{cm}{W}\right) = \frac{2\sqrt{2}\Delta T}{L_{eff} I} \tag{6}$$

where

$$|\Delta\varphi| = \frac{\Delta T_{p-v}}{0.406(1-S)^{0.25}} \tag{7}$$

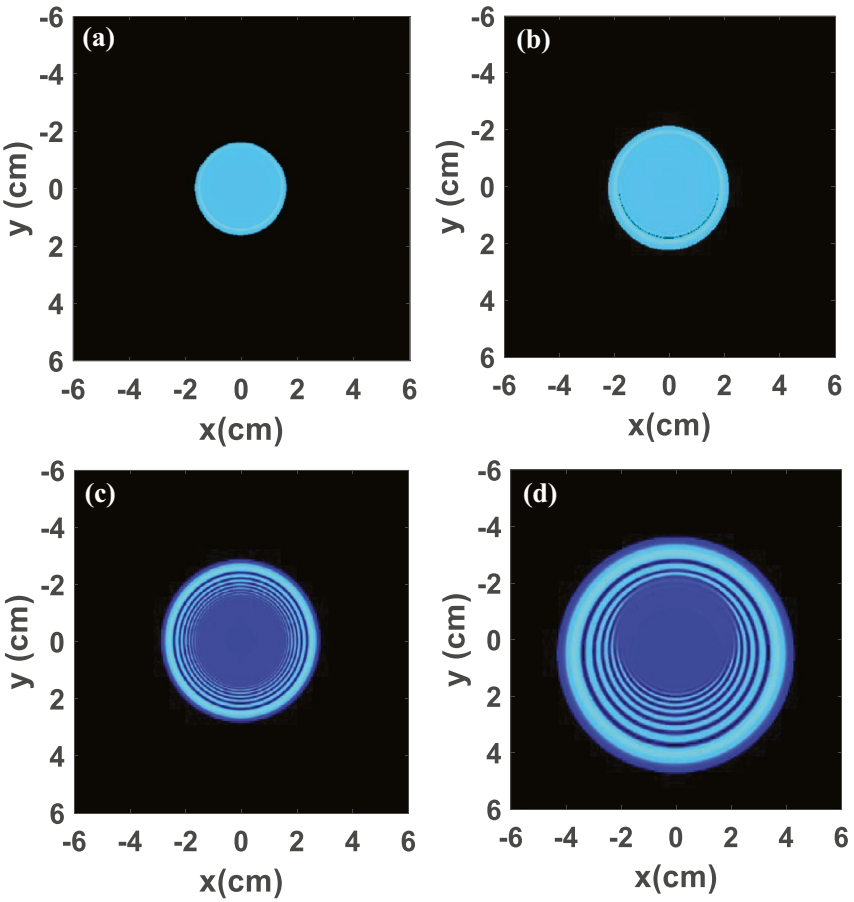

Fig. 14 Theoretically calculated variations of far field diffraction patterns on the power input at the far field (mW): **a** 17, **b** 27, **c** 42, **d** 61 in the mixture of PU and NR dye solution

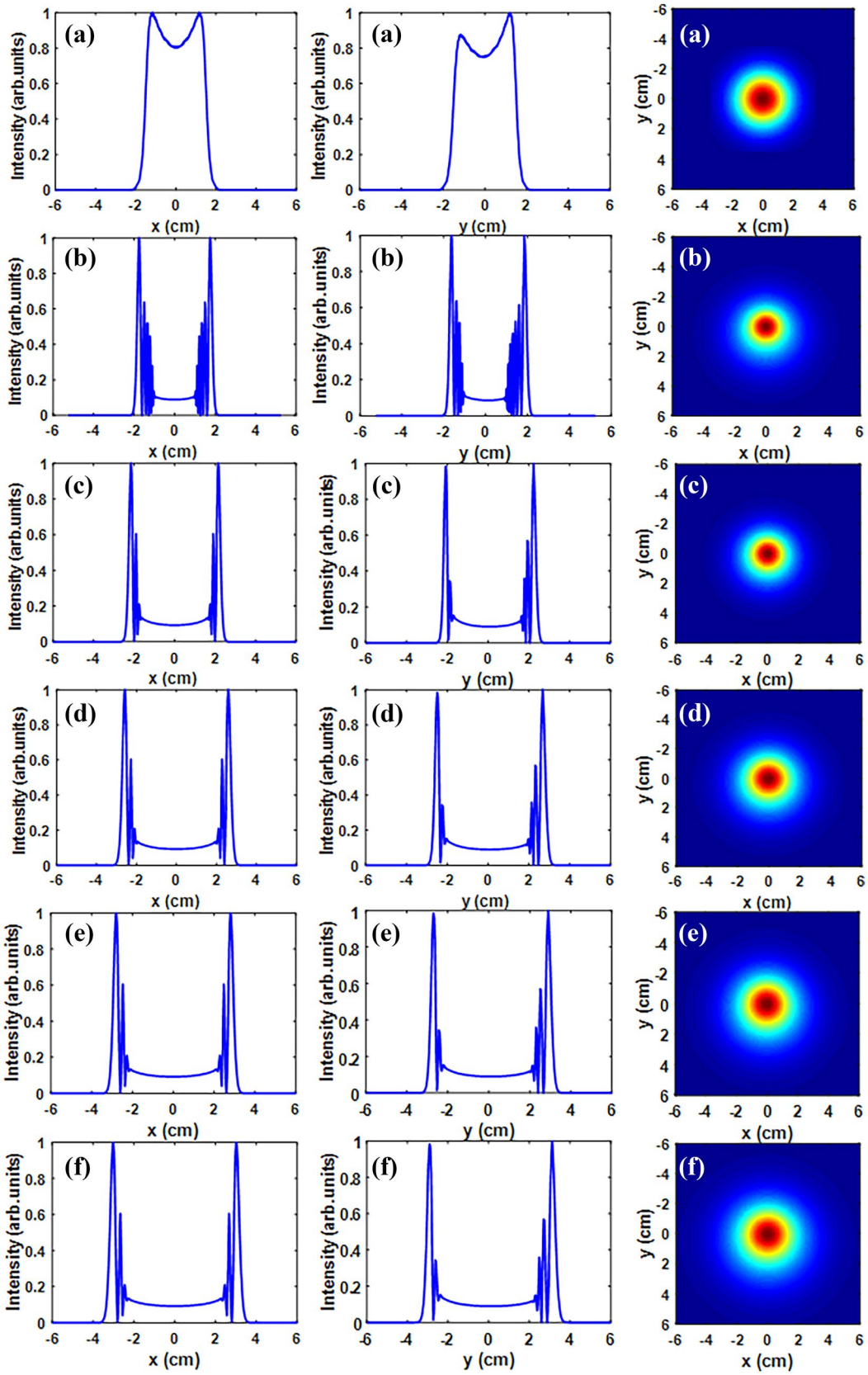

Fig. 15 Theoretically calculated temporal variations of the laser light amplitude in the x-direction (**C1**), y- direction (**C2**) and 2d phase change of beam. (**C3**) at power input of 61 mW in the mixture of PU and NR dye solution (msec): **a** 0, **b** 100, **c** 200, **d** 500, **e** 850, **f** 1000

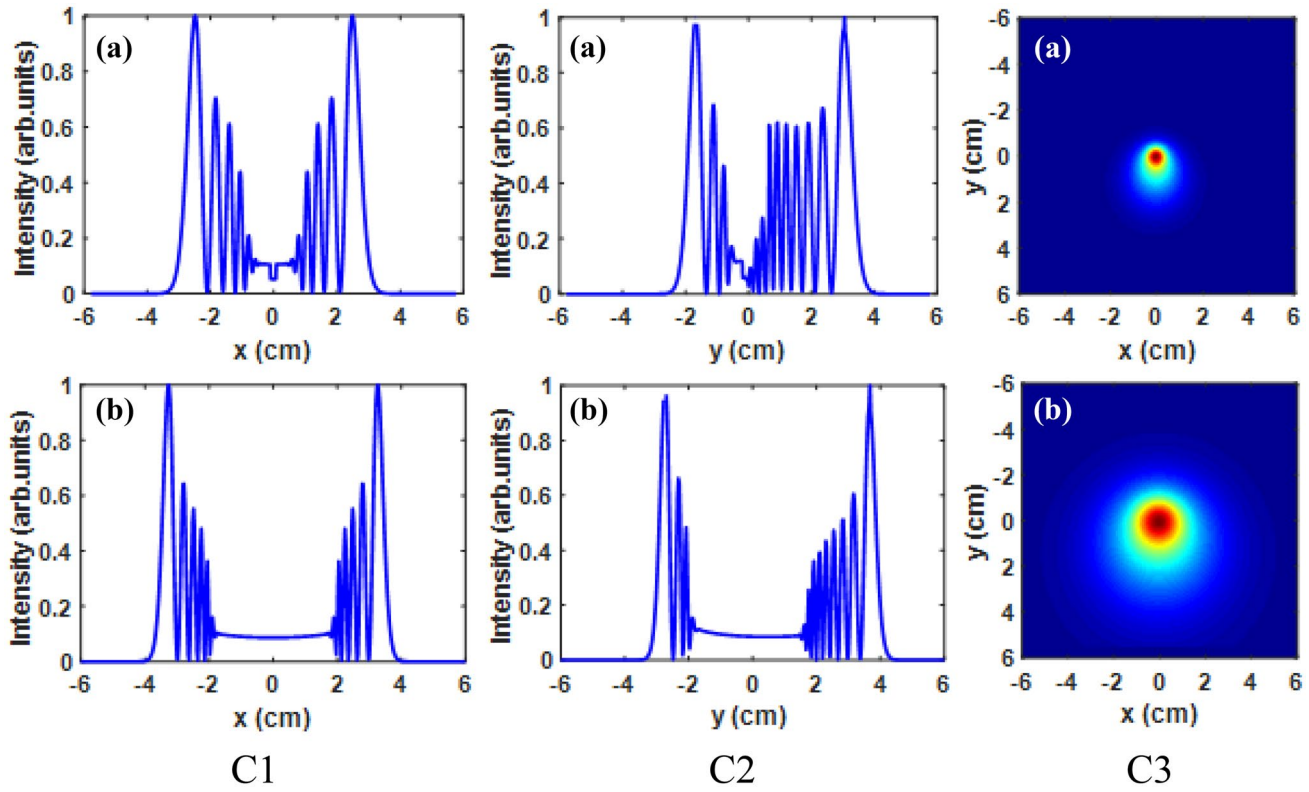

Fig. 16 Theoretically calculated effect of wave front on the laser light amplitude in the x- direction (**C1**), y- direction (**C2**) and 2d phase of laser beam variation (**C3**) at power input of 61 mW, first raw for convex beam and second raw for concave beam in the mixture of PU and NR dye solution

$$L_{eff} = \left[1 - \exp(-\alpha d)\right]/\alpha \tag{8}$$

$$\Delta T_{p-v} = T_p - T_v \tag{9}$$

$$S = 1 - \exp\left(-\frac{2r_a^2}{\omega_a^2}\right) \tag{10}$$

$$\Delta T = 1 - T_p \tag{11}$$

where $\Delta\varphi$ (dimensionless) is the on axis beam phase shift,L_{eff} (cm) is the effective sample thickness, ΔT_{p-v} (dimensionless) is peak difference between peak (T_p) (dimensionless) and valley (T_v) (dimensionless) transmittance of the CA: Z-scan data, ω_a (cm) is the beam radius at the aperture,S (dimensionless) is the aperture transmittance, r_a (cm) is the radius aperture and ΔT is one minus the peak value transmittance (T_p) in the OA: Z-scan figure. By using the Eqs. (5)–(11) and the values of ΔT and ΔT_{p-v} from the Fig. 8a, c and with $P = 5$ mW, the values of β and n_2 equals to 4.89×10^{-3} cm/W and 3.09×10^{-7} cm^2/W respectively for mixture of PU and NR dye solution.

Evaluation of the Limiting Threshold of the Sample

To determine the limiting threshold, T_H, of an optical limiter one can draw the relation between the laser beam transmittance through the sample and power input that is shown in Fig. 11. T_H is the power input value as the medium transmittance reduced to half its maximum value, from Fig. 11, we find that the sample's transmittance decreases to half when the input power is 10.5 mW, so the limiting threshold value, T_H, for the mixture PU and NR dye solution is 10.5 mW and for beam radius of 1 cm, corresponds to the intensity of 6.69×10^{-3} W/cm^2.

Modeling of Diffraction Patterns

In the presence of a cw Gaussian beam with intensity profile passing through the mixture of PU and NR dye solution diffraction patterns generated, Figs. 5, 6 and 7, where

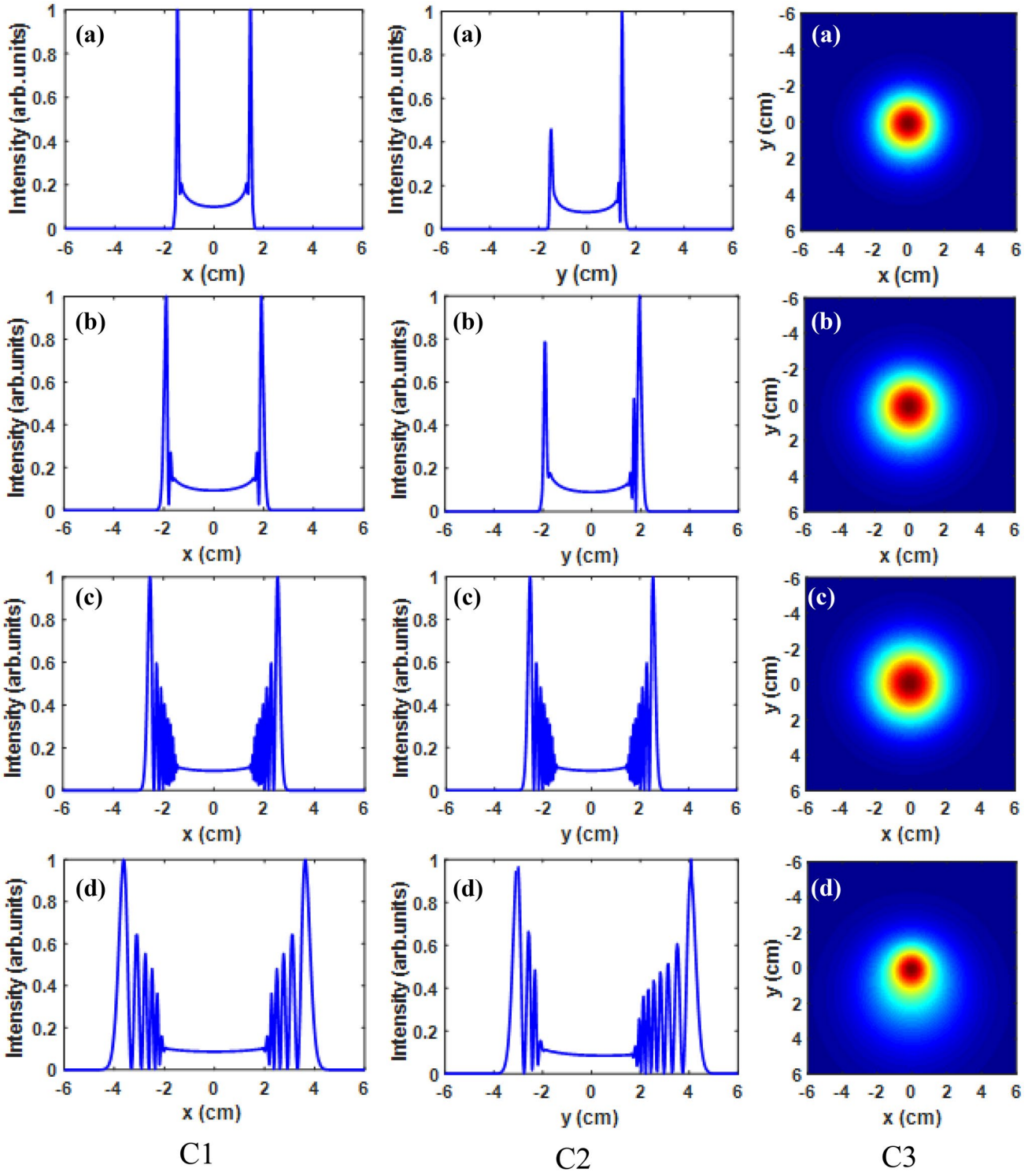

Fig. 17 Theoretically calculated input power effect on the laser light amplitude in the x- direction (**C1**). y- direction (**C2**) and 2d phase variations of laser beam (**C3**) in the mixture of PU and NR dye solution: (mW) **a** 17 mW, **b** 27 mW, **c** 42 mW, **d** 61

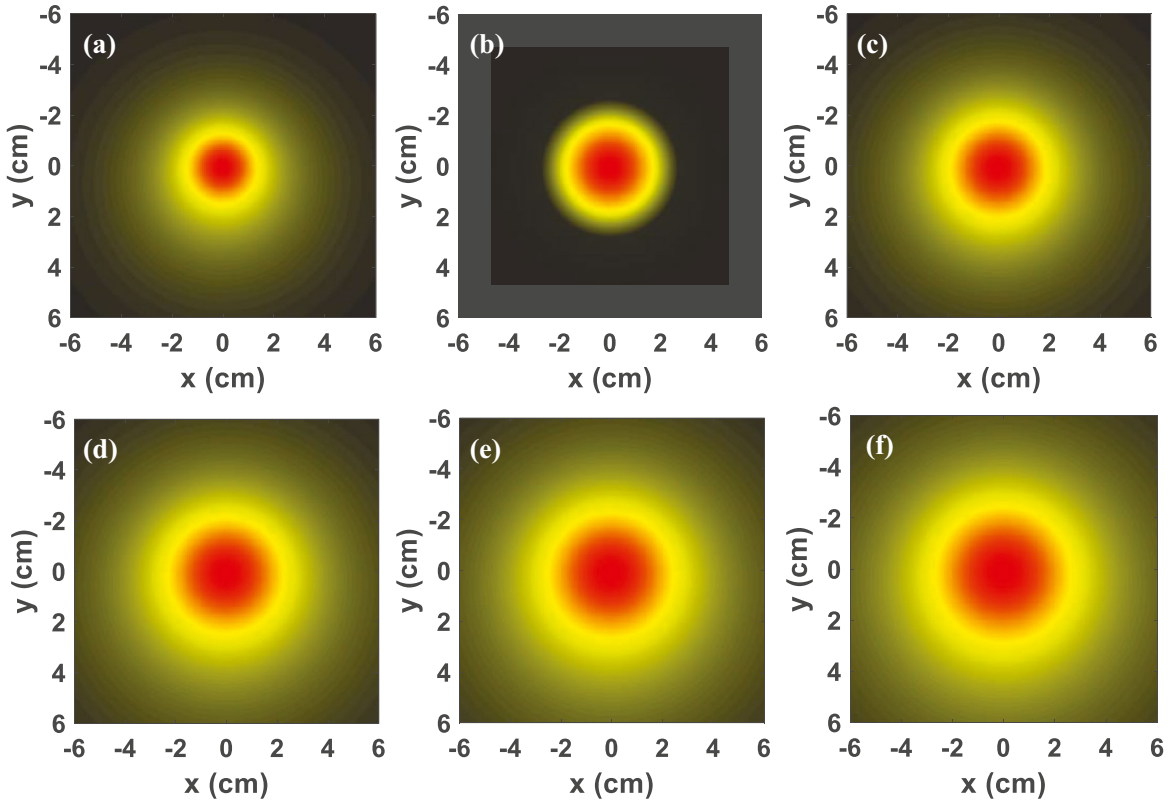

Fig. 18 Theoretically calculated temporal 2-dimensional variations of tempearture (msec) **a** 0, **b** 100, **c** 200, **d** 500, **e** 800, **f** 1000 in the mixture of PU and NR dye solution at 61 mW

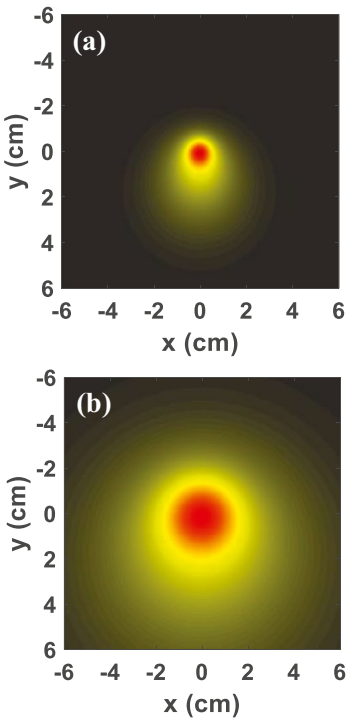

Fig. 19 Theoretically calculated wave front effect on the 2 dimensional distribution variations of tempruture **a** convex beam and **b** concave beam, in the mixture of PU and NR dye solution at 61 mW

the type of patterns depends on the laser beam wave front and on time. As the beam enters the sample cell part of its energy is absorbed. The amount of absorption depends on the medium absorption coefficient, which leads to generation of heat locally in the shape of Gaussian profile by non-radiation decays. The temperature of the medium will be maximum at the peak of the Gaussian beam so that the change of the medium refractive index will be maximum so that the medium acts as a concave lens that work on the increasing the area of the laser beam due to self-defocusing that distort the beam wavefront. The PU doped with NR solution refractive index will be affected as a result. The amount of the variation of the refractive index, n(x,y,t),depends on the amount of temperature change, $\Delta T(x, y, t)$,which will change the beam phase, $\Delta\varphi(x, y, t)$. It was seen in Fig. 5, 6 and 7, the patterns lose symmetry as input power increased and as time increased due to the thermal convection current vertically when it is larger than the horizontal conduction current. In the experiments,the screen distance from the sample, L, spatial coordinates (x,y) are rewritten as (x', y'). Based on the Fraunhofer approximations to the F.K. integral, the laser beam intensity distribution $I(x', y', t)$ (W/cm.^{2}) post traversing the mixture of PU and NR dye solution cell on thedetector or the screen can be written as follows [51, 52]:

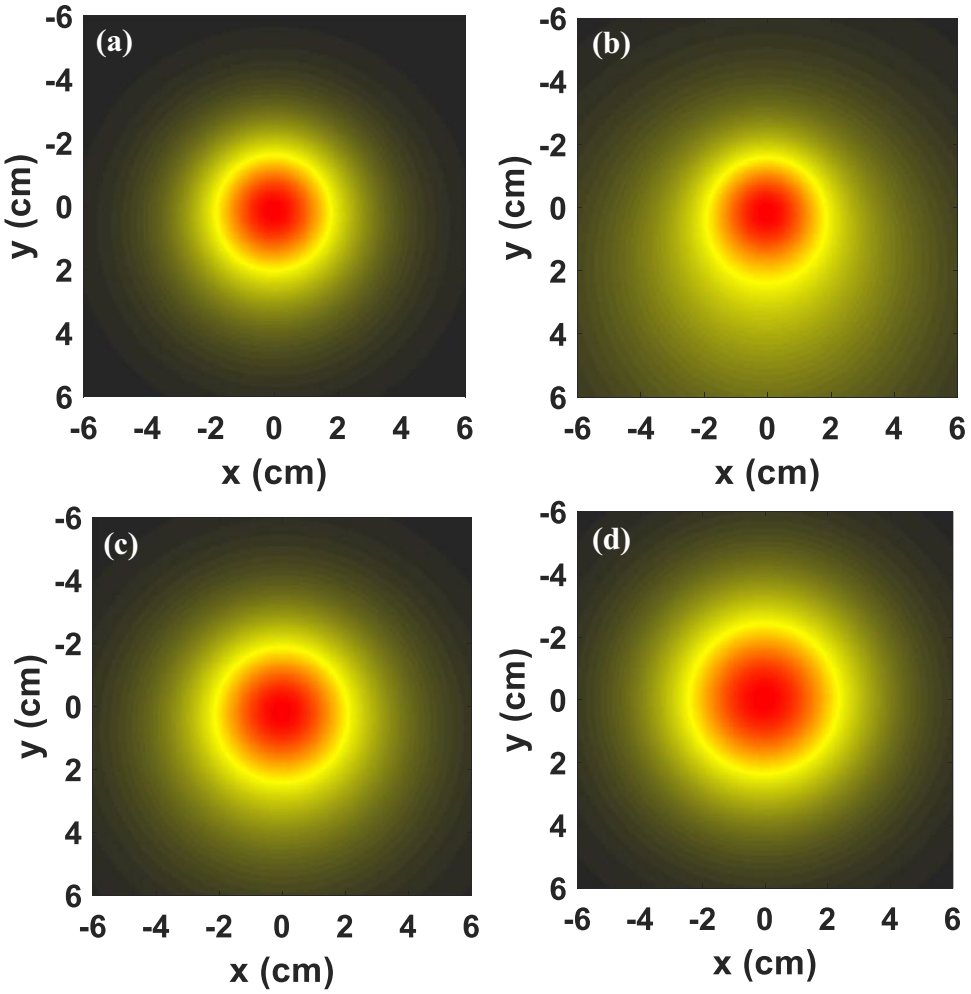

Fig. 20 Theoretically calculated power input effect on the 2 dimensional distribution variations of temperature (mW) **a** 17, **b** 27, **c** 42 **d** 61 of in the mixture of PU and NR dye solution

$$I(\acute{x},\acute{y},t) = \left|\left(\frac{2P}{\pi\omega^2}\right)^{\frac{1}{2}} \frac{i\pi\omega^2}{\lambda L}.\exp(ikL).\exp\left(\frac{-\alpha d}{2}\right)\int_{-\infty}^{\infty} dx \int_{-\infty}^{\infty} dy.\exp\left(\frac{x^2+y^2}{\omega^2}\right)^2 .\exp\left[i\left(-k\frac{x^2+y^2}{2R}+\triangle\varphi(x,y,t)\right)\right]\exp\left(\frac{-ik(x\acute{x}+y\acute{y})}{L}\right)\right| \tag{12}$$

L, ω, λ, d, and R are taken in cm, α in cm^{-1}, P in W, and Δφ is dimensionless. Equation (12) was solved using the Mat Lab system, the results are shown in Figs. 12, 13, 14, 15, 16, 17, 18, 19 and 20. Figure 12 represents the calculated temporal variations of a chosen diffraction pattern, Fig. 13 represents the calculated dependent of the type of diffraction patterns on the type of beam wave front. Figure 14 represents the calculated dependence of diffraction pattern on input power, Figs. 15, 16 and 17 represent calculated laser light amplitude along the x- and y-directions, and the two dimensional variations of the light phase in the cases of Figs. 12, 13 and 14 respectively. Figures 18, 19 and 20 represents the calculated variations of the medium temperatures in two dimension for the cases of Figs. 12, 13 and 14, while Fig. 21 shows direct comparison between specific cases chosen exprimentally and theoretically with good accord obtained.

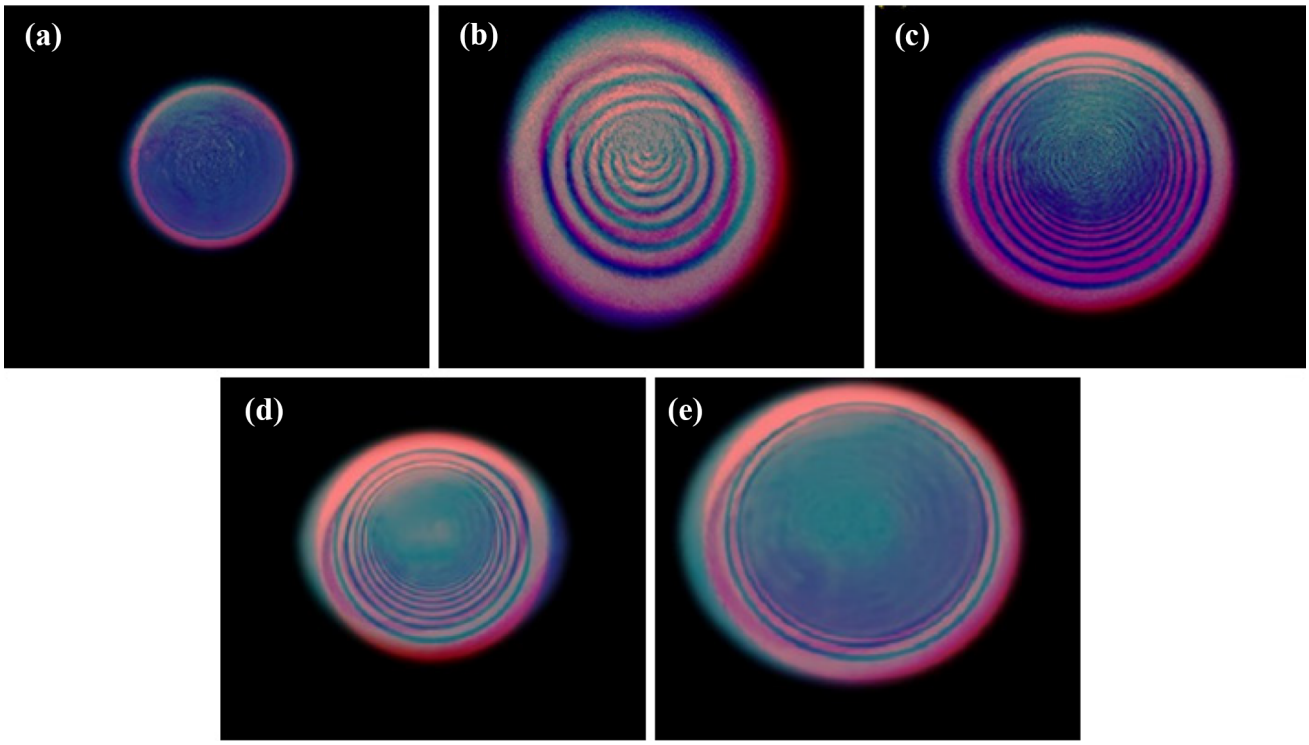

Fig. 21 Comparison of the theortical (red) and experimental (blue) diffraction patterns in the mixture of PU and NR dye solution for the cases: **a** 18 mW input, **b** convex and, **c** concave beams at 61 mW **d** 100 ms at 61 mW, **e** 1000 ms at 61 mW

Conclusion

The interaction of a 473 nm continuous wave laser beam with the mixture of polyurethane and neutral red dye solution leded in the generation of diffraction patrens. Based on the number of diffraction patterns and the Z-scan, both the nonlinear refractive index and nonlinear absorption coefficient respectively were determined. Good accord between the experimentel findings of diffraction patterns and the numerically obtained one via the use of Fresnell-Kirchoof integral were obtained. Optical limiting preporty was tested in the sample at wavelength 473 nm with limiting threshold of 10.5 mW was obtained. The passage of 473 nm and 532 nm beams have led to the all-optical switching phenomena in the prepared sample.

Authors' Contributions Kh. A. Al-Timimy and H. A. Sultan wrote the manuscript, Qusay M. A. Hassan participated in the characterization and analysis of the results, C. A. Emshary wrote the main manuscript text – review & editing and Ali Qassim Abdullah and Emad Abdul Reaz Arebi prepared Figs. 1, 2 and 3. All authors reviewed the manuscript.

Availability of Data and Materials The authors confirm that the data supporting the findings of this study are available within the article.

Declarations

Ethics Approval and Consent to Participate The authors declare that their commitment to ethics related to his work and they have designed the experiments, collected and analyzed the data, and written the manuscript.

Consent for Publication The authors declare their consent of publication.

Competing Interests The authors declare that they have no known competing financial interests or personal relationships that could have appeared to influence the work reported in this paper.

References

1. Potember RS, Hoffman RC, Stetyick KA, Murphy RA (1988) Molecular materials for nonlinear optics. John Hopkin APL Techno Dig 9:189–198
2. Halasyamani SP, Zhang W (2017) Viewpoint inorganic material, for UV and Leep-UV nonlinear optical applications. Inorg Chem 56:12077–12085
3. Khoo IC (1994) Liquid crystal nonlinear optics. Act Phys Polon A 86:267–134
4. Linke Li, Yang H, Song Y, Hou H, Fan Y (2006) Two cobalt(II) one-dimensional ribbon of rings polymers: Synthesis, structures and non-linear optical properties. Inorg Chim Acta 359:2135–2140

5. Jiang L, Lu F, Gao Y, Song Y, Liu H, Gan H, Jiu T, Li Y, Li Y, Wang S, Zhu D (2006) Nonlinear optical properties of an ultrathin film containing porphyrin and poly (phenylenevinylene) units. Thin Solid Films 496:311–316
6. Shi FW, Meng XJ, Wang GS, Sun JL, Lin T, Ma JH, Li YW, Chu JH (2006) The third-order optical nonlinearity of $Bi_{3.25}La_{0.75}Ti_3O_{12}$ ferroelectric thin film on quartz. Thin Solid Films 496:333–335
7. Alsous MB, Zidan MD, Ajji Z, Allahham A (2014) Z-scan measurements of optical nonlinearity in acid blue 29 dye. Optik 125:5160–5163
8. Zidan MD, Allaf AW, Alsous MB, Allahham A (2014) Investigation of optical nonlinearity and diffraction ring patterns of carbon nanotubes. Opt Las Technol 58:128–134
9. Zidan MD, Al-Ktaifani MM, El-Daher MS, Allahham A, Ghanem A (2020) Diffraction ring patterns and nonlinear measurements of the Tris (2′, 2-bipyridyl) iron (II) tetrafluoroborate. Opt Las Technol 131:106449
10. Hassan QMA, Palanisamy PK, Manickasundaram S, Kannan P (2006) Sudan IV dye based poly(alkyloxymethacrylate)films for optical data storage. Opt Commun 267:236–243
11. Manickasundaram S, Kannan P, Hassan QMA, Palanisamy PK (2008) Azo dye based poly(alkyloxymethacrylate)s and their spacer effect on optical data storage. J Mater Sci Mater Electron 19:1045–1053
12. Manickasundaram S, Kannan P, Kumaran R, Velu R, Ramamurthy P, Hassan QMA, Palanisamy PK, Senthil S, Narayanan SS (2011) Holographic grating studies in pendant xanthene dyes containing poly(alkyloxymethacrylate)s. J Mater Sci Mater Electron 22:25–34
13. Kagami M (2004) Visible optical fiber communication. R&D Rev Toyota 40:1–6
14. Hassan QMA, Manshad RKH (2019) Surface morphology and optical limiting properties of azure B doped PMMA film. Opt Mater 92:22–29
15. Hassan QMA, Manshad RKH (2015) Optical limiting properties of sudan red B in solution and solid film. Opt Quant Electron 47:297–311
16. Al-Mudhaffer MF, Al-Ahmad AY, Hassan QMA, Emshary CA (2019) Optical characterization and all-optical switching of benzenesulfonamide azo dye. Optik 127:1160–1166
17. Durbin SD, Arakelian SM, Shen YR (1981) Laser-induced diffraction rings from a nematic liquid-crystal film. Opt Lett 8:411–413
18. Franko M, Tran CD (2010) Thermal lens spectroscopy, Encyclop. Analy. Chem. R. A. Meyers (Ed) John Wiley and Sons Ltd. 1–32
19. Derkowska-Zielinska B, Barwiolek M, Cassagne C, Boudebs G (2020) Nonlinear optical study of Schiff bases using Z-scan technique. Opt Las Technol 124:105968 (7pp)
20. Callen WR, Hutth BG, Pantell RH (1967) Optical patterens of thermally self -defocused light. Appl Phys Lett 11:103–105
21. Sheik-Bahae M, Said AA, Van Stryland EW (1989) High sensitivity single beam n_2 measurements. Opt Lett 14:955–957
22. Sheik-Bahae M, Said AA, Wei T, Hagan DJ, Van Stryland EW (1990) Sensitive measurement of optical nonlinearities using a single beam. IEEE J Quant Electron 26:760–769
23. Shabeeb GM, Emshary CA, Hassan QMA, Sultan HA (2020) Investigating the nonlinear optical properties of poly eosin-Y phthalate solution under irradiation with low power visible CW laser light. Phys B 578:411847 (13pp)
24. Sultan HA, Hassan QMA, Bakr H, Al-Asadi AS, Hashim DH, Emshary CA (2018) Thermal-induced nonlinearities in rose, linseed and chamomile oils using CW visible laser beam. Can J Phys 96:157–164
25. Hassan QMA, Emshary CA, Sultan HA (2021) Investigating the optical nonlinear properties and limiting optical of eosin methylene blue solution using a cw laser beam. Phys Scr 96:095503 (16 pp)
26. Emshary CA, Hassan QMA, Bakr H, Sultan HA (2021) Determination of the optical constants, nonlinear optical parameters and threshold limiting of methyl red-epoxy resin film. Phys B 622:413354 (8 pp)
27. Al-Timimy KhA, Hassan QMA, Sultan HA, Emshary CA (2020) Solvents effect on the optical nonlinear properties of the sudan iv. Optik 224:165398 (15 pp)
28. Abdulkader AF, Hassan QMA, Al-Asadi AS, Bakr H, Sultan HA, Emshary CA (2018) Linear, nonlinear and optical limiting properties of carbon black in epoxy resin. Optik 160:100–108
29. Jebur JH, Hassan QMA, Al-Mudhaffer MF, Al-Asadi AS, Elias RS, Saeed BA, Emshary CA (2020) The gamma radiation effect on the surface morphology and optical properties of alphamethyl curcumin: PMMA film. Phys Scr 95:045804 (10pp)
30. Khalaf SK, Hassan QMA, Emshary CA, Sultan HA (2022) Concentration effect on optical properties and optical limiting of PVA doped with nigrosin films. J Photochem Photob A Chem 427:113809 (11 pp)
31. Kadhum AJ, Hussein NA, Hassan QMA, Sultan HA, Al-Asadi AS, Emshary CA (2018) Investigating the nonlinear behavior of cobalt (II) phthalocyanine using visible CW laser beam. Optik 157:540–550
32. Elias RS, Hassan QMA, Emshary CA, Sultan HA, Saeed BA (2019) Formation and temporal evolution of diffraction ring patterns in a newly prepared dihydropyridone. Spectrochim Acta Part A Mol Biomol Spectrosc 223:117297 (16 pp)
33. Saeed BA, Hassan QMA, Emshary CA, Sultan HA, Elias RS (2020) The nonlinear optical properties of two dihydropyridones derived from curcumin. Spectrochim Acta Part A Mol Biomol Spectrosc 240:118622 (14 pp)
34. Almashal FA, Mohammed MQ, Hassan QMA, Emshary CA, Sultan HA, Dhumad AM (2020) Spectroscopic and thermal nonlinearity study of a Schiff base compound. Opt Mater 100:109703 (12 pp)
35. Jassem AM, Hassan QMA, Emshary CA, Sultan HA, Almashal FA, Radhi WA (2021) Synthesis and optical nonlinear properties performance of azonaphthol dye. Phys Scr 96:025503 (20 pp)
36. Sultan HA, Dhumad AM, Hassan QMA, Fahad T, Emshary CA, Raheem NA (2021) Synthesis, characterization and the nonlinear optical properties of newly synthesized 4-((1,3-dioxo-1-phenylbutan-2-yl)diazenyl) benzenesulfonamide. Spectrochim Acta Part A Mol Biomol Spectrosc 251:119487 (15 pp)
37. Mutlaq DZ, Hassan QMA, Sultan HA, Emshary CA (2021) The optical nonlinear properties of a new synthesized azo-nitrone compound. Opt Mater 113:110815 (13 pp)
38. Dhumad AM, Hassan QMA, Emshary CA, Fahad T, Raheem NA, Sultan HA (2021) Nonlinear optical properties investigation of a newly synthesised Azo-(β)- diketone dye. J Photochem Photobio A Chem 418:113429 (17 pp)
39. Dhumad AM, Hassan QMA, Fahad T, Emshary CA, Raheem NA, Sultan HA (2021) Synthesis, structural characterization and optical nonlinear properties of two azo- β-diketones. J Mol Struct 1235:130196 (9 pp)
40. Al-Hamdani UJ, Hassan QMA, Emshary CA, Sultan HA, Dhumad AM, Al-Jaber AA (2021) All optical switching and the optical nonlinear properties of 4-(benzothiazolyldiazenyl)-3-chlorophenyl 4-(nonylthio)benzoate (EB-3Cl). Optik 248:168196 (17 pp)
41. Hassan QMA, Raheem NA, Emshary CA, Dhumad AM, Sultan HA, Fahad T (2022) Preparation, DFT and optical nonlinear studies of a novel azo-(β)- diketone dye. Opt Las Technol 148:107705 (14 pp)
42. Abdullmajed HA, Sultan HA, Al-Asadi RH, Hassan QMA, Ali AA, Emshary CA (2022) Synthesis, DFT calculations and optical nonlinear properties of two derived Schiff base compounds from ethyl-4-amino benzoate. Phys Scr 97:025809 (18 pp)

43. Jia Y, Shan Y, Wu L, Dai X, Fan D, Xiang Y (2018) Broad band nonlinear optical resonance and all-optical switching of liquid phase exfoliated tungsten diselenide. Phot Res 6:1040–1046
44. Waang Q, Wu X, Wu L, Xiang Y (2019) Broadband nonlinear optical response in Bi_2Se_3-Bi_2Te_3 heterastructure and it's application in all-optical switching. AIP Adv 9:025022 (7 pp)
45. El-Fadl AA, Mohamad GA, El-Moiz ABA, Rashad M (2005) Optical constants of $Zn_{1-x}Li_xO$ films prepared by chemical bath deposition technique. Phys B 366:44–54
46. Santamato E, Shen YR (1984) Field-curvature effect on the diffraction ring patterns of a laser beam dressed by spatial self-phase modulation in a nematic film. Opt Lett 9:564–566
47. Deng L, He K, Zhon T, Li C (2005) Formation and evolution of far-field diffraction patterns of divergent and conver Gaussian beams passing through self-focusing and self-defocusing media. J Opt Aipure Appl Opt 7:409–415
48. Shan Y, Tang J, Wa L, Ln S, Dain X (2014) Spatial self-phase nodulation and all-optical switching of graphene oxciz dimensional martials. J Cent South Univ 26:2295–2306
49. Jia Y, Liao Y, Wu L, Shan Y, Dai X, Cai H, Xiang Y, Fan D (2019) Nonlinear optical response, all optical switching, and all optical information conversion in NbSe2 nanosheets based on spatial self-phase modulation. Nanoscale 11:4515–4522
50. Ogusu K, Kohtani Y, Shao H (1996) Laser-induced diffraction rings from an absorbing solution. Opt Rev 3:232–234
51. Karimzadeh R (2012) Spatial self-phase modulation of a laser beam propagation through liquids with self-induced natural convection flow. J Opt 14:095701 (9 pp)
52. Karimzadeh R (2013) Studies of spatial self-phase modulation of a laser beam passing through liquids. Opt Commun 286:329–333